An Experimental Study of UWB Device-Free Person Detection and Ranging

Yakup Kilic*, Henk Wymeersch†, Arjan Meijerink*, Mark J. Bentum*, William G. Scanlon*‡

*University of Twente, The Netherlands, E-mail: {y.kilic, a.meijerink, m.j.bentum, w.g.scanlon}@utwente.nl
†Chalmers University of Technology, Sweden, E-mail: henkw@chalmers.se
‡The Queen's University of Belfast, U.K., E-mail: w.scanlon@qub.ac.uk

Abstract—**Passive person detection and localization is an emerging area in UWB localization systems, whereby people are not required to carry any UWB ranging device. Based on experimental data, we propose a novel method to detect static persons in the absence of template waveforms, and to compute distances to these persons. Our method makes very little assumptions on the environment and can achieve ranging performances on the order of 50 cm, using off-the-shelf UWB devices.**

I. INTRODUCTION

Ultra-wide bandwidth (UWB) transmission is a promising technology for wireless localization, due to its high-resolution ranging and obstacle penetration capabilities [1], [2]. Most practical UWB localization systems rely on targets (e.g., objects, people) to carry an active UWB device. However, tracking people and assets even without requiring them to be equipped with any radio-frequency (RF) device is a desired capability in some application areas (e.g., smart environments, intruder detection, emergency response and elderly care). Traditional techniques such as infrared motion detectors and video camera surveillance are limited to visible line of sight (LOS) [3], whereas RF-based techniques overcome this problem [4]. Among others, UWB signals are attractive for device-free person detection and localization because of the superior time resolution, which makes it possible to distinguish reflections due to the static objects in the environment from those due to the human target.

UWB was demonstrated as an effective technique for human-being detection through respiratory movement of the person in [5], [6]. Recently, experimental demonstrations were also given for MIMO UWB [7], different antenna polarizations [8], and sensing of the person through obstructions [9]. With the aim of estimating respiration and heart rates, an analytical framework was developed in [10], and related Cramér–Rao lower bounds were calculated in [11]. In [12], a channel model was introduced for breathing detection and human-target ranging. While these works focused on the detection of static people from breathing information, human-body detection and tracking were also studied experimentally for moving people in an open area in [13], [14] and behind walls in [15]. Most of these studies consider mono-static radars where the transmitter and the receivers are co-located, and detection relies on the back-propagation of the signal from the body. Object tracking in UWB sensor networks was studied in [16], which derived Cramér–Rao lower bounds, assuming a specular reflection model. Finally, imaging of environments and objects based on an UWB transmission was considered in [17], [18], and signal analysis methods were developed in [19]. However, very little work has been done in the case when transmitter and receiver are not co-located, and there is no unified signal processing methods to detect, range, and localize people. In [20], a novel UWB device-free person detection and localization technique has been proposed to detect the presence of a static person without requiring any prior knowledge of the environment. The method relies on capturing slow temporal variations induced by the person, as seen by UWB devices that are not co-located, and is robust against wideband background noise.

In this experimental study, we present the essence of the device-free detection method, that is corroborated with observations from a set of indoor UWB experiments. We also introduce a new device-free ranging approach which extracts the traveling distance of the reflection from a suitable detection statistic. The performance of both detection and ranging techniques are shown based on the UWB experiments, conducted in an indoor environment for different transmitter, receiver and the person positions.

The remainder of this paper is organized as follows. In Section II, we introduce the signal model and describe the device-free detection and ranging techniques in Section III and Section IV, respectively. In Section V, experimental results are provided before we draw conclusions in Section VI.

II. SIGNAL MODEL

A. Experimental Observations

We consider a scenario where a UWB transmitter and a UWB receiver are separated by a distance of R meters in an indoor LOS environment, and a person standing on an ellipse (considering the position of the person as a point at the center of the body) with focal points at transmitter and receiver positions and major axis length $(R + \delta)$ meters (or, equivalently, a delay of δ/c with respect to the arrival instant of the direct-path signal, where c denotes the speed of light). We transmit N_{rep} waveforms from the transmitter to the receiver and align the N_{rep} received waveforms by postprocessing in the delay domain, starting from the arrival time of the signal.

View in the delay domain: Fig. 1 shows the mean of $N_{\text{rep}} = 100$ received UWB waveforms, collected with off-the-shelf UWB radios, when a person is present (dashed line)

43
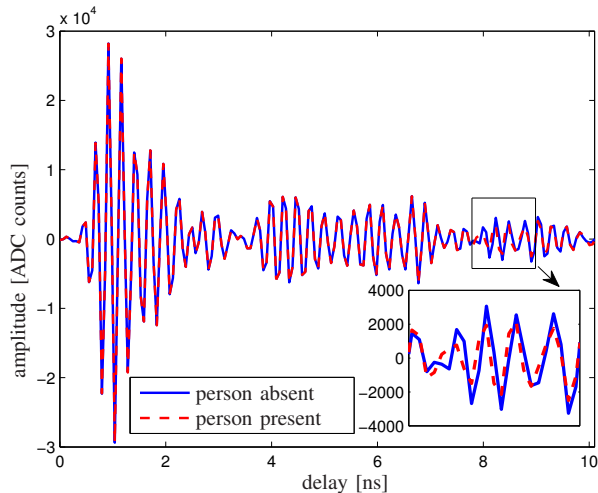
Fig. 1. Mean of 100 UWB measurements, taken continuously within 20 seconds in an indoor LOS environment, in the absence (solid line) and the presence (dashed line) of a person.

Fig. 2. Evolution of the received waveform over time at delay instant 8.3 ns, in the absence and presence of a person.

or absent (solid line). The person was standing on an ellipse corresponding to $\delta/c = 7.9$ ns. We observe that the signal is affected by the person to some extent starting from 7.6 ns after the first arrival. However, the difference between the two signal means is small, therefore without a clean template signal (i.e., in the same environment, in the absence of the person), it is hard to determine the signal changes due to the person.

View in the time domain: Fig. 2 offers a different perspective, and shows the variation of the signal over the $N_{\rm rep}$ repetitions at a fixed delay of 8.3 ns (i.e, zeroth delay instant corresponds to the arrival time of the signal), in the presence and the absence of the person. We note that the $N_{\rm rep}$ repetitions corresponds to an observation time of 20 seconds. It is clear that, without a person, the signal show only little variation around 3000 analog-to-digital converter (ADC) counts, as it is mainly affected by the noise. In contrast, when the person is present, the signal shows more significant variations, albeit slowly over time, even in a fixed position. This effect can be explained through suitable propagation models [10], [11], capturing minor temporal variations induced by, amongst others, the breathing of the person. Here, we will not go into complex propagation models, but rather view the signal in Fig. 2, in the presence of the person, as a generic low-frequency signal plus background noise.

B. Mathematical Model

Our observations lead us to pose the following signal model. The transmitter sends $N_{\rm rep}$ copies of a ranging symbol [2]

$$s(t) = \sqrt{\frac{E_{\rm s}}{N_{\rm f}}} \sum_{j=0}^{N_{\rm f}-1} p_j w(t - jT_{\rm f} - c_j T_{\rm c}), \qquad (1)$$

where $E_{\rm s}$ denotes the energy of the symbol, $p_j \in \{\pm 1\}$ is the polarity code, $T_{\rm f}$ is the duration of the frame and $N_{\rm f}$ is the number of pulses in the symbol, $w(t)$ denotes the unit energy
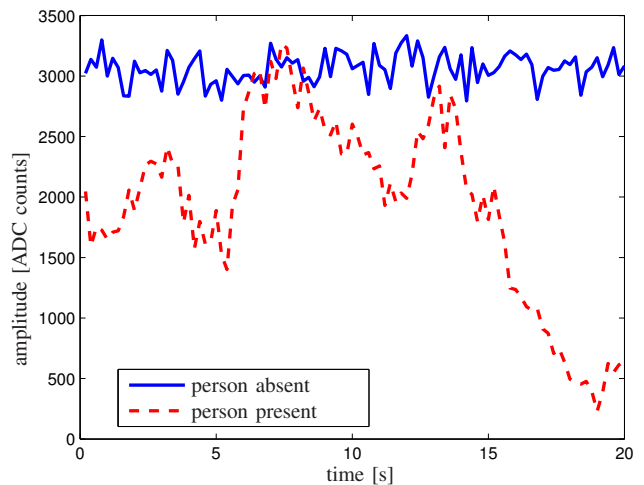
UWB pulse of duration $T_{\rm w} < T_{\rm f}$, $c_j \in \{0, 1, \ldots, N_{\rm h}-1\}$ is the time-hopping code, T_c and $N_{\rm h}$ are the chip duration and the number of chips per frame, respectively. The total duration of the symbol is $T_{\rm s} = N_{\rm f} T_{\rm f}$, being smaller than the delay spread of the channel. The receiver coherently combines $N_{\rm f}$ pulses during each of the $N_{\rm rep}$ repetitions, leading to the following received signal

$$r_{\rm rep}(t) = \sqrt{E_{\rm s}} \sum_{k=1}^{N_{\rm rep}} \sum_{l=1}^{L} \alpha_l w(t - \tau_l - kT_{\rm s})$$

$$+ \sqrt{E_{\rm s}} \sum_{k=1}^{N_{\rm rep}} \alpha_{\rm p}(t) w(t - \tau_{\rm p} - kT_{\rm s}) + n(t) \qquad (2)$$

where we assumed L resolvable signal reflections with corresponding channel gains α_l and delays τ_l, as well as one resolvable signal component due to the presence of a person, with delay $\tau_{\rm p}$ and slowly varying channel gain $\alpha_{\rm p}(t)$. The noise $n(t)$ is assumed to be white with power spectral density $N_0/2$. Direct sampling of $r_{\rm rep}(t)$ at a sufficiently high rate W, where $T_{\rm s}W$ is assumed to be an integer, and aligning the $N_{\rm rep}$ copies, we obtain a two-dimensional model, with $r(kT_{\rm s}, m/W) = r_{\rm rep}(kT_{\rm s} + m/W)$, $\alpha_{\rm p}(kT_{\rm s}, m/W) = \alpha_{\rm p}(kT_{\rm s} + m/W)$ and $n(kT_{\rm s}, m/W) = n(kT_{\rm s} + m/W)$ for $k = 1, 2, \ldots, N_{\rm rep}$ and $m = 0, 1, \ldots, T_{\rm s}W - 1$:

$$r(kT_{\rm s}, m/W) = \sqrt{E_{\rm s}} \sum_{l=1}^{L} \alpha_l w(m/W - \tau_l)$$

$$+ \sqrt{E_{\rm s}} \alpha_{\rm p}(kT_{\rm s}, m/W) w(m/W - \tau_{\rm p})$$

$$+ n(kT_{\rm s}, m/W), \qquad (3)$$

with

$$\mathbb{E}\{n(kT_{\rm s}, m/W)n(k'T_{\rm s}, m'/W)\} =$$

$$\frac{N_0 W}{2} \delta(k - k')\delta(m - m'). \qquad (4)$$

where $\mathbb{E}\{.\}$ denotes the statistical expectation and $\delta(.)$ is the discrete delta function. In view of our model, the second term in (3) again corresponds to the person, which introduces a single channel coefficient that varies slowly over time (i.e., as a function of k). Finally, the received signal-to-noise ratio, which is defined as SNR $= 2E_{\rm s}/N_0$, is dependent on the number of pulses (i.e determining the duration of the ranging symbol $T_{\rm s}$) as $E_{\rm s}$ scales proportional to the number of pulses. Therefore, there is a trade-off between the received SNR and the number of repetitions $N_{\rm rep}$ possible in a unit time.

C. Receiver Operation

Assuming the delays are ordered such that τ_1 corresponds to the propagation delay of the direct LOS path and $\tau_{\rm p}$ is the delay of the reflection from the person, the receiver operates in the following order:

1) **Ranging:** Estimate τ_1, using a standard time-of-arrival techniques [1];
2) **Person detection:** Detect whether a person is present;
3) **Device-free ranging:** If a person is present, estimate $\tau_{\rm p}$; and
4) **Delivery:** Deliver an estimate of $(\tau_{\rm p} - \tau_1) \times c$ as the device-free range to the localization application.

In the subsequent sections, we will describe how to perform tasks 2) and 3). The localization application collects device-free ranges between multiple pairs of devices. Each device-free range corresponds to an ellipse, and the position of the person can be found from the intersection of those ellipses, using, for instance, a least squares estimator.

III. Detection

Considering a fixed sample delay $m \in \{0, 1, \ldots, T_{\rm s}W - 1\}$ in (3), we can plot the resulting signal as a function of k, and would obtain signals as shown in Fig. 2. The terms in (3), that do not vary with time, do not convey any relevant information for our purpose. They can be found by averaging over time, and then subtracted. Hence, we obtain the following simplified signal model

$$r_m(k) = \begin{cases} n_m(k), & \text{no person affects delay } m \\ x_m(k) + n_m(k), & \text{person affects delay } m, \end{cases} \tag{5}$$

where the delay index m is moved to the subscript to emphasize the dependence on the time dimension k and $x_m(k)$ denotes an arbitrary low-frequency signal induced by the person. The received signal can be further decomposed as

$$r_m(k) = r_{m,\rm L}(k) + r_{m,\rm H}(k). \tag{6}$$

where $r_{m,\rm L}(k)$ and $r_{m,\rm H}(k)$ are the low- and the high-frequency components, with fractional bandwidths of β and $1 - \beta$, respectively, where $\beta \ll 1$. Fractional bandwidths are obtained by normalizing the bandwidth to $1/T_{\rm s}$. Stacking samples for different $k \in \{1, \ldots, N_{\rm rep}\}$ into a vector, we can obtain $\mathbf{r}_m$, $\mathbf{x}_m$, and $\mathbf{r}_{m,\rm L}$. Then, we obtain a likelihood ratio

test that yields a test statistic

$$\Lambda_m = \frac{p(\mathbf{r}_m | \text{person affects delay } m)}{p(\mathbf{r}_m | \text{no person affects delay } m)} \tag{7}$$

$$= \frac{\exp\left(-\frac{1}{N_0 W} \|\mathbf{r}_m - \mathbf{x}_m\|^2\right)}{\exp\left(-\frac{1}{N_0 W} \|\mathbf{r}_m\|^2\right)} = \exp\left(\frac{2\mathbf{r}_m^T \mathbf{x}_m - \|\mathbf{x}_m\|^2}{N_0 W}\right)$$

Note that, even though $\mathbf{x}_m$ is unknown, we treat it as a deterministic vector in the likelihood ratio test and replace it with an estimate. Since, we are only interested in the low-pass nature of $\mathbf{x}_m$, the estimate is set to $\hat{\mathbf{x}}_m = \mathbf{r}_{m,\rm L}$. After normalization with $\beta N_{\rm rep}$, a final statistic can be obtained for a single delay index m as

$$y(m) = \frac{\|\mathbf{r}_{m,\rm L}\|^2}{N_0 \beta W N_{\rm rep}} \tag{8}$$

where, in the absence of the person, $\mathbb{E}\{y(m)\} = 1$. Assuming that the person has an effect over the duration of the transmitted signal $T_{\rm w}$, information over multiple delays can be aggregated by averaging the delay-specific statistic over a window around a trial delay τ, which is assumed to be an integer multiple of $1/W$:

$$D(\tau) = \frac{1}{T_{\rm w}W} \sum_{m=(\tau - T_{\rm w}/2)W}^{(\tau + T_{\rm w}/2)W} y(m). \tag{9}$$

The presence of a person can thus be determined by comparing $D(\tau)$ to a threshold as

$$\begin{cases} D(\tau) \leq \gamma & \text{no person present for delay } \tau \\ D(\tau) > \gamma & \text{person present for delay } \tau, \end{cases} \tag{10}$$

where γ is a threshold that can be selected based on the desired performance. The analytical derivation of the false alarm and the miss detection probabilities are given in [20].

IV. Device-Free Ranging

Once a person is detected, we propose two methods to estimate $\tau_{\rm p}$ from (3).

1) Line Search: Since the decision statistic developed in (10) conveys information over the presence of the person and the delay of the reflection, we can obtain an estimate of $\tau_{\rm p}$ by simply employing a maximum value search as

$$\hat{\tau}_{\rm p} = \arg \max_{\tau \in [0, T_{\rm s}]} D(\tau). \tag{11}$$

2) Threshold Crossing: Although the line search method works well in some conditions, we observed experimentally that, in some other cases, the decision statistic $D(\tau)$ has multiple peaks. The first of these peaks corresponds to the person, and needs not always correspond to the maximum of $D(\tau)$. This phenomenon is a shortcoming of our simple model, and manifests itself especially when the transceivers and/or the person are close to strong reflectors (e.g., walls, metallic objects) in the environment. In this case, not only the paths that are directly reflected off the person, but also the ones that are reflected off the body and the reflectors in the
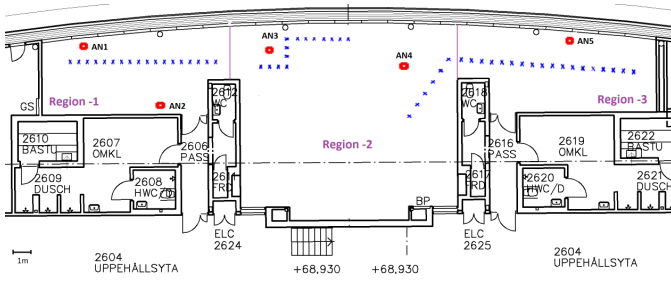
Fig. 3. Overview of the measurement floor-plan: The floor was divided into three regions and for each region the person was standing on several positions (shown as blue crosses) while anchors (shown as red squares for AN1 to AN5) were having ranging measurements in such a way that, for each position of the person, the measurements were initiated in between AN1 and AN2 (Region 1), AN3 and AN4 (Region 2), and AN4 and AN5 (Region 3).

Fig. 4. Examples of the measured decision statistic $D(\tau)$ as a function of delay: Case-I (blue line) with $R = 6.66$ m and the true device-free range 6.7 m (black cross), and Case-II (dashed red line) with $R = 7.85$ m and true device-free range 9.77 m. The device-free range estimates with Threshold Crossing and Line Search are shown as a black rectangular and a black circle, respectively.

environment (in other words indirect reflections), show slow fluctuations over time. Similar observations are also obtained for the case when the person is standing in the vicinity of the transmitter and the receiver. Note that, as these indirect reflections travel over a longer path, they will always arrive later than signal components that are directly reflected off the person.

These observations lead us to introduce a threshold-based approach, where the delay related to the person corresponds to the first threshold crossing:

$$\hat{\tau}_{\mathrm{p}} = \min\left\{\tau : D(\tau) > \tilde{\gamma}\right\}. \tag{12}$$

Note that $\tilde{\gamma}$ may be set to a different value than γ, depending on the desired performance and false alarm criteria.

V. EXPERIMENTAL RESULTS

In this section, we quantify the performance of the proposed device-free person detection and ranging techniques based on the results of an indoor UWB measurement campaign.

A. Overview of the Experiment Setup

We performed UWB measurements inside a fitness room on the campus of Chalmers University of Technology. Measurements were performed with identical and commercially-available UWB radio units (Time Domain Corp. P400 RCM module), equipped with omni-directional UWB antennas within the devices' operating frequency range of 3–5.5 Ghz. The radios are capable of conducting two-way time-of-arrival ranging transactions and provide range estimate as well as a received waveform with a sampling time of 61 ps over a window of approximately 10 ns,[1] limiting the maximum captured multi-path length to be less than approximately 3 m. In other words, given the distance between the transmitting and the receiving anchors as R m, with the current radios the person can be only detected within an ellipse whose focal points are the anchor positions and whose major axis length is $(R + 3)$ m. After measuring with a high-sampling rate

[1]In some cases, it is possible to capture the waveforms longer than 10 ns, however, with the current hardware the waveform becomes unstable beyond 10 ns, making it meaningless to process the received signal across the time.

oscilloscope, the transmitted pulse duration was found to be approximately 1.4 ns, resulting in approximately $T_{\mathrm{w}}W = 23$ samples in the delay dimension.

As shown in Fig. 3, the fitness room was divided into three parts. Five radios, serving as anchors, were placed in these regions. The person was standing in 18, 20, and 18 different positions, separated by 50 cm, and for each position we established transmission between AN1 and AN2, AN3 and AN4, and AN5 and AN4, respectively, in Region 1, Region 2 and Region 3. Mapping the environment in a coordinate system, we calculated the exact positions of the anchors and the person, with the aid of a laser distance measurement tool. Although the measurement plan is presented in a two-dimensional space in Fig. 3, anchors were positioned at different heights of 0.54 m (AN1), 2.66 m (AN2), 0.73 m (AN3), 0.64 m (AN4) and 0.97 m (AN5). Moreover, the antenna-to-antenna distances between the anchors were approximately 5.68 m, 6.66 m and 7.85 m for the pairs of AN1-AN2, AN3-AN4, and AN5-AN4, respectively. The waveforms were collected with a rate M_{rate} of 50 measurements/second, allowing us to obtain 100 snapshots over 2 seconds for each position of the person. During the measurements, care was taken to keep the environment static such that there was no other person within the device-free range limited by radios (i.e, the operator, who was carrying out the experiments, was also outside of this range). During the off-line post-processing, we performed fine alignment of the waveforms around the leading edge point (by means of cross-correlation) to make sure that all the waveforms were aligned over the time window. The starting instant of the waveform (i.e., the zero delay instant) is defined based on the leading edge detection point, obtained by the radio.

Finally, we estimate the noise power N_0 on a delay-by-
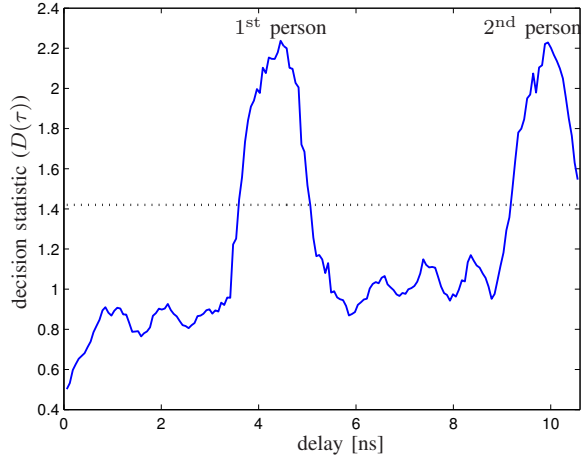
Fig. 5. An example of the measured decision statistic $D(\tau)$ as a function of delay for two persons, with $R = 6.66$ m, and true device-free ranges of 7.3 m (first person) and 9.7 m (second person). The threshold is shown indicated by the dotted line.

delay basis to account for the imperfections introduced in time domain such as timing jitter.[2] For a delay index m, the noise power spectral density $N_{0,m}$ is estimated as

$$\hat{N}_{0,m} = \frac{1}{W(1-\beta)N_{\text{rep}}} \sum_{k=1}^{N_{\text{rep}}} r_{m,\text{H}}^2(k), \qquad (13)$$

where $r_{m,\text{H}}(k) = r_m(k) - r_{m,\text{L}}(k)$ is the part of the signal that is due to the noise, regardless of the presence of the person. We then substituted the estimate in (8) to allow detection and ranging in the presence of hardware imperfections.

B. Results and Discussion

1) Decision Statistic: Before providing detailed results on the detection rates and ranging errors, we first consider the decision statistic. Fig. 4 shows an example of the measured decision statistic $D(\tau)$, where the subject was standing on two different positions. Since the noise power is dependent on the delay (due to the timing jitter) and gets lower values for lower signal amplitudes, the decision statistic gets high values for the delay values where the signal has a slowly varying component (also due to the indirect reflections) with low amplitude. This can be clearly observed for Case- I in Fig. 4. The threshold crossing method can easily deal with this effect. When the person is away from the direct path between the anchors, only one distinct peak is visible (see Case- II in Fig. 4), and the line search yields an estimate close to the threshold crossing method.

We also performed experiments with two human subjects. In some of these experiments, two persons are clearly distinguishable in the decision statistic, an example of which is shown in Fig. 5. Based on the positions of the peaks in the

[2]Timing jitter causes different amounts of background noise for the delay samples with high signal amplitudes compared to the ones with low signal amplitudes.

Fractional Bandwidth	Measurement Duration [sec]	Missed Det. Rate
0.1	2	0.04
	1.6	0.07
	1.2	0.13
	0.8	0.27
	0.4	0.69
0.2	2	0.02
	1.6	0.18
	1.2	0.29
	0.8	0.38
	0.4	0.67
0.5	2	0.09
	1.6	0.69
	1.2	0.82
	0.8	0.89
	0.4	1

decision statistic, the device-free range errors are 0.7 m and 0.05 m for the first and second person, respectively.

2) Detection: The operator stood on the 56 unique positions, as indicated in Fig. 3. Of those 56 positions, 10 were out of the device-free range. For the remaining 46 positions, Table I shows the missed detection rates, for different values of the fractional bandwidth of the filter ($\beta \in \{0.1, 0.2, 0.5\}$, or absolute bandwidths of 5 Hz, 10 Hz and 25 Hz, respectively) and the observation duration in the time dimension ($N_{\text{rep}} \times M_{\text{rate}}$, corresponding to durations of 2, 1.6, 1.2, 0.8 and 0.4 seconds). We chose the detection thresholds that allow the false alarm probability of approximately 10^{-5}, based on the numerical results given in [20].

Results reveal that the missed detection rate increases for higher values of the fractional bandwidth. This is due to the fact that we collect more noise energy when we increase the bandwidth of the filter, resulting in lower values for the decision statistic. On the other hand, the missed detection rate is inversely proportional to the measurement duration. This shows that the slow variations due to the movement of the static person result in enough energy at the output of the low-pass filter, for instance, for 2 seconds of measurement time in most cases. In contrast, short durations (e.g., 0.4 seconds), are not sufficient to detect the body-induced slow variations. These results may also be linked to the physical properties of the person, where the body can be considered to be approximately motion-less at the sub-second scale (i.e., no noticeable effect of the respiration on the movement of the chest cavity). Therefore, there is a trade-off between the update rate of the system and the extent of detecting the presence of the person.

3) Device-free Ranging: To visualize the device-free ranging performance, we consider the three regions from Fig. 3 separately. In each region, the distance between the transmitting and receiving anchor is fixed, and we vary the position of the operator, for the case where $\beta = 0.1$ and the observation duration is 2 seconds. These parameters are chosen since we
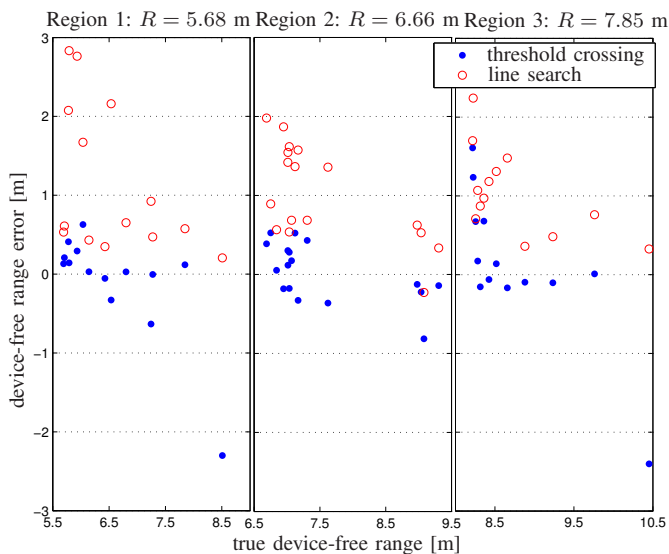
Fig. 6. Device-free range error versus true device-free range for the Threshold Crossing (blue dot) and Line Search (red circle) methods, with anchor distances of 5.68 m (leftmost), 6.66 m (center) and 7.85 m (rightmost), $\beta = 0.1$ and a measurement duration of 2 seconds.

get high detection performance (see Table I). The results are shown in Fig. 6, for the 44 positions where the presence of the person is detected. The results reveal that, in general, threshold crossing outperforms the line search method, with root-mean squared errors (averaged over 44 measurement points) of 0.67 m and 1.28 m, respectively. As expected, the line search yields positively biased estimates. For most of the cases, the absolute error for the threshold crossing method is less than 65 cm. The performance difference between the ranging methods is particularly noticeable when the person is standing close to the direct line (i.e., the shortest distance between the antennas) between the anchors, as already discussed in relation to Fig. 4.

VI. CONCLUSION AND FUTURE WORK

We proposed a novel technique to perform device-free detection and ranging of static people. Our method is based on the slow temporal variations in the UWB signal, induced by slight movements of the person, and does not require any prior knowledge of the environment. Based on an experimental campaign with off-the-shelf UWB radios, we were able to demonstrate the device-free detection and ranging performance of the system. Our results indicate that the proposed technique could be also applicable to cases with multiple people. Future works include investigating the effects of the other moving objects on detection and ranging techniques, development of ranging error models, locating multiple people, and tracking of moving people.

ACKNOWLEDGEMENT

REFERENCES

[1] C. Falsi, D. Dardari, L. Mucchi, and M. Z. Win, "Time of arrival estimation for UWB localizers in realistic environments," *EURASIP J. on Applied Signal Processing*, vol. 2006, pp. 1–13, 2006, special issue on *Wireless Location Technologies and Applications*.
[2] S. Gezici, Z. Tian, G. B. Giannakis, Z. Sahinoglu, H. Kobayashi, A. F. Molisch, and H. V. Poor, "Localization via ultra-wideband radios," *IEEE Signal Process. Mag.*, vol. 22, no. 4, pp. 70–84, July 2005.
[3] T. Teixeira, G. Dublon, and A. Savvides, "A survey of human-sensing: Methods for detecting presence, count, location, track, and identity," *ACM Comput. Surveys*, vol. 5, issue 1, pp. 59–69, 2010.
[4] N. Patwari, J. Wilson, "RF sensor networks for device-free localization: Measurements, models, and algorithms," *Proc. IEEE*, vol. 98, no. 11, pp. 1961–1973, Nov. 2010.
[5] A. G. Yarovoy, L. P. Ligthart, J. Matuzas, and B. Levitas, "UWB radar for human being detection," *IEEE Aerosp. Electron. Syst. Mag.*, vol. 21, no. 3, pp. 10–14, March 2006.
[6] G. Ossberger, T. Buchegger, E. Schimback, A. Stelzer, and R. Weigel, "Non-invasive respiratory movement detection and monitoring of hidden humans using ultra wideband pulse radar," in *Proc. 2004 Int. Workshop on Ultra Wideband Systems, Joint with Conf. on Ultrawideband Systems and Technologies (Joint UWBST & IWUWBS).*, 18–21 May 2004, pp. 395-399.
[7] Y. Xu, S. Wu, J.Shao, J. Chen, and G. Fang, "Life detection and by MIMO Ultra wideband radar," in *Proc. 2012 14th Int. Conf. on Ground Penetrating Radar (GPR)*, 4–8 June 2012, pp. 80-84.
[8] A. Nezirovic, S. Tesfay, A. S. E. Valavan, and A. Yarovoy, "Experimental study on human breathing cross section using UWB impulse radar ," in *Proc. 2008 European Radar Conf. (EuRAD)*, 30–31 Oct. 2008, pp. 1-4.
[9] J. Sachs, M. Helbig, R. Herrmann, M. Kmec, K. Schilling, and E. Zaikov, "Remote vital sign detection for rescue, security, and medical care by ultra-wideband pseu-do noise radar," Ad Hoc Netw. (2012), http://dx.doi.org/10.1016/j.adhoc.2012.07.002.
[10] S. Venkatesh, C. R. Anderson, N. V. Rivera, R. M. Buehrer, "Implementation and analysis of respiration-rate estimation using impulse-based UWB," in *Proc. 2005 IEEE Military Comm. Conf. (MILCOM)*, 17–20 Oct. 2005, pp. 3314-3320.
[11] S. Gezici and Z. Sahinoglu, "Theoretical limits for estimation of vital signal parameters using impulse radio UWB," in *Proc. 2007 Int. Conf. on Comm. (ICC)*, 24–28 June. 2007, pp. 5751-5756.
[12] V. Casadei, N. Nanna, and D. Dardari, "Experimental study in breath detection and human target ranging in the presence of obstacles using ultra-wideband signals," *Int. J. Ultra Wideband Communications and Systems*, vol. 2, no. 2, pp. 116–123, 2011.
[13] S. Chang, N. Mitsumoto, and J. W. Burdick, "An algorithm for UWB radar-based human detection," in *Proc. 2009 IEEE Radar Conf. (Radar-Con)*, Pasadena, CA, May 2009, pp. 1-6.
[14] S. Chang, R. Sharan, M. Wolf, N. Mitsumoto, and J. W. Burdick, "UWB radar-based human target tracking," in *Proc. 2009 IEEE Radar Conf. (RadarCon)*, Pasadena, CA, May 2009, pp. 1-6.
[15] J. Li, Z. Zeng, J. Sun, and F. Liu, "Through-wall detection of human beings movement by UWB radar," *IEEE Geosci. Remote Sens. Lett.*, vol. 9, no. 6, pp. 1079–1083, Nov. 2012.
[16] C. Chang, and A. Sahai, "Object tracking in a 2D UWB sensor network," in *Proc. 38th Asimolar Conf. Signals Syst. Comput.*, Nov 2004, pp. 1252-1256.
[17] R. Thomä, O. Hirsch, J. Sachs, and R. Zetik, "UWB sensor networks for position location and imaging of objects and environments," in *Proc. 2nd Eur. Conf. Antennas Propag.*, 2007, pp. 1–9.
[18] W. Guo, N. P. Filer, and R. Zetik, "Indoor mapping and positioning using impulse radios," in *Proc. IEEE/ION Position Location Navigat. Symp.*, 2006, pp. 153-163.
[19] J. Shen, and A. F. Molisch, "Discerning direct and indirect paths: Principle and application in passive target positioning systems," in *Proc. Global Commun. Conf. (Globecom 2011)*, 2011, pp. 1–6.
[20] Y. Kilic, H. Wymeersch, A. Meijerink, M. J. Bentum, and W. G. Scanlon, "Device-free person detection and ranging in UWB networks," submitted to *IEEE J. Sel. Topics Signal Process.*, special issue on *non-cooperative localization networks* [Online]. Available: http://arxiv.org/abs/1303.4092.